

Exact method of determination of the recombination mode from time resolved photoluminescence data

Pawel Strak¹, Kamil Koroński², Kamil Sobczak³, Jolanta Borysiuk⁴, Krzysztof P. Korona⁴, Konrad Sakowski¹, Andrzej Suchocki², Eva Monroy⁵, Agata Kaminska^{2,6} and Stanislaw Krukowski¹

¹*Institute of High Pressure Physics, Polish Academy of Sciences, Sokolowska 29/37, 01-142 Warsaw, Poland*

²*Institute of Physics Polish Academy of Sciences, Al. Lotników 32/46, 02-668 Warsaw, Poland*

³*Faculty of Chemistry, Biological and Chemical Research Centre, University of Warsaw, Zwirki i Wigury 101, 02-089 Warsaw, Poland*

⁴*Faculty of Physics, University of Warsaw, Pasteura 5, 02-093 Warsaw, Poland*

⁵*Université Grenoble-Alpes, CEA, INAC-Pheliqs, 17 av. des Martyrs, 38000 Grenoble, France*

⁶*Cardinal Stefan Wyszyński University, College of Science, Department of Mathematics and Natural Sciences, Dewajtis 5, 01-815 Warsaw, Poland*

A method of data analysis is proposed for the determination of the carrier recombination processes of optically excited matter measured by time-resolved photoluminescence, differentiating monomolecular, bi-molecular, tri-molecular, and higher order molecular processes. Our method allows to determine whether the so-called ABC model describes time evolution of optical relaxation of the excited system. The procedure is applicable to the time evolution of any optically excited medium. As an illustration, the method is successfully applied to III-nitride polar and non-polar multi-quantum wells. We show that in this case the mono- and bi-molecular process determine the carrier relaxation, and the tri-molecular Auger recombination contribution is negligible.

I. Introduction

Application of photoluminescence (PL) and its time resolved version (TRPL) constitutes significant part of the present day investigations of the properties of such diverse systems as single atoms, molecules, solids, and whole class of quantum confined systems, such as quantum wells, rods and dots. The PL measurements explore electronic states of the system therefore they were developed relatively early.^{1,2} As the amount of potential information is enormous, the PL measurement techniques steadily progressed, extending their scope and functionalizing their application using different modifications and improvements.³

Among the adopted features, TRPL is one of the most important and productive.^{3,4} In the TRPL measurements, nonequilibrium occupation of a portion of quantum states is induced which is then relaxed towards equilibrium. For extended systems, the nonequilibrium density of the electrons and holes (e-h) is created by the initial laser impulse which then/next relax by their recombination. Part of the recombination processes entail emission of photons (i.e. radiative recombination) which are measured by optical detectors. The deexcitation processes without emission of photons contribute to non-radiative recombination. All the types of recombination may involve a single, a pair, or more carriers; they are called mono-, bi-, tri-molecular, etc. processes. The recombination decreases density of excess, nonequilibrium carriers. Thus the time evolution of the excess carrier density may be studied by measurements of time evolution of the PL intensity. The solutions exist for each separate molecular type process, thus the single process could be distinguished easily.⁴ In reality, the several types of recombination are entangled at the same time and their deconvolution is difficult, giving various results. Thus the direct and unambiguous PL time evolution analysis method does not exist in practice.

In practical analysis of the experimental results it is assumed that the time decay of the optical emission of highly optically excited semiconductor medium can be divided into monomolecular, bi-molecular, tri-molecular and possibly higher order molecular processes.¹⁻⁵ The monomolecular decay may contain contribution of several recombination modes, including nonradiative recombination, related to presence of defects, known as Shockley-Read-Hall (SRH) recombination⁶, and also Wannier-Mott exciton recombination.^{7,8} Contribution of the single and collective excitons is dominant for low temperatures⁹, i.e. at the conditions of majority of PL experiments. However for high electron densities, the excitons are screened or even decomposed so they do not play the most important role.^{10,11}

Additionally, for recombination in the multiquantum wells (MQWs), the escape from the wells may contribute to monomolecular decay.¹² Several physical mechanisms may lead to recombination outside QWs, including lack of electron capture in the wells, electron escape, asymmetry of electron and hole transport in semiconductors, p-type doping of electron blocking layer (EBL) in semiconductor structures, etc.¹³ In many cases, additional investigations such as temperature or pressure dependence in combination with *ab initio* calculations¹⁴ are therefore necessary to disentangle the different contributions to monomolecular processes. It has to be also noted that division of the recombination channels into mono-, bi-, tri-, and higher molecular recombination modes does not entail precise identification of the nature of the recombination process. Thus several recombination processes may contribute the global recombination rate of the single molecular process type.

The radiative recombination, especially in semiconducting materials, may be related to band-to-band recombination, direct or indirect, which may be associated either with monomolecular or bi-molecular recombination, depending on the condition of the experiment.¹⁵ The observed PL time decay may be additionally affected by the energy transfer by exchange mechanism, involving defects.^{16,17} For example, in research of nitride structures, the peculiar behavior of PL intensity from $\text{In}_x\text{Ga}_{1-x}\text{N}$ ($0 < x < 0.25$) layers and MQWs was explained by Chichibu localization model, according to which, the carrier are localized in high In content regions, and isolated from dislocations, which constitute the non-radiative recombination channels.^{18,19} As it was confirmed experimentally,^{20,21} the localization works at low excitations, hence it is expected that even at higher excitations, during the time evolution, the transition from non-localized to localized recombination mode may change the results. In addition, the built-in and piezo induced electric fields in the wells²¹⁻²³ may affect the recombination by at least two different mechanisms: field induced dissociation of the excitons and energy shift due to screening change related to time dependent density of the electric charge.²⁵ This is verified below by comparative studies on polar and nonpolar GaN/AlN MQWs.

The most prominent example of the tri-molecular or higher molecular processes is Auger recombination. The process involves nonradiative transfer of excess energy created due to e-h recombination to the third carrier (electron or hole) which is ejected from its original state.^{26,27} Depending on the final state of the ejected carrier, several types of the Auger processes were identified: internal, external, etc. The Auger recombination was recently identified as the most likely phenomenon responsible for efficiency droop^{28,29}, i.e. relative

decrease of light emission of nitride light emitting diodes (LEDs) under high injection current, known for recent 15 years.^{30,31} The Auger coefficients were hard to determine, their measurements were burdened by influence of e-h ratio, electric field, or hot carrier escape.³² As a result, Auger coefficient may vary by one or even two orders of magnitude, which can be also related to its determination via indirect efficiency measurement.²⁹ Thus precise, independent assessment of magnitude of Auger processes contribution in e-h recombination, and determination of Auger coefficient is very needed.

The purpose of this work is to present a new method of analysis of temporal evolution of PL intensity, based on logarithmic derivative method. The method allows to identify the mono-, bi- and tri- molecular and higher order decay of excitation by the optical emission. Examples of applications are shown demonstrating the power of the method. The perspectives of application in basic research and also of application in characterization of structures and devices are described.

II. Theoretical background

Time-resolved PL experiments proceed via excitement of the semiconductor sample by intensive laser pulse. The energy of the laser radiation is such that a photon can generate a single electron-hole (e-h) pair in the conduction and the valence band, respectively. The generated excess density of electrons $n(t_o)$ and holes $p(t_o)$ at the time of the pulse t_o is

$$n(t_o) = n_{tot}(t_o) - n_{eq} \quad (1a)$$

$$p(t_o) = p_{tot}(t_o) - p_{eq} \quad (1b)$$

where the suffixes 'tot' and 'eq' denote total and equilibrium density of the carriers, respectively. Each photon generates an e-h pair, so that $n(t_o) = p(t_o)$. After the pulse, during the PL emission process ($t > t_o$), the e-h pairs are annihilated. Therefore, for negligible carrier escape, we can write $n(t) = p(t)$ for $t > t_o$.

The *radiative recombination* process, which generates the PL signal, proceeds either by exciton or free carrier annihilation, in both cases involving an e-h pair, i.e. it is a bi-molecular process. Thus, the radiative recombination rate reflects the bi-molecular character of the process:

$$R_{rad}^b(t) = B^b n_{tot}(t) p_{tot}(t) \quad (2)$$

where B^b ($B^b > 0$) is a proportionality constant.

On the other hand, *SRH recombination* is a nonradiative monomolecular process related to the presence of the defects. Photogenerated carriers are captured at the defect site and then they gradually relax towards the opposite band (ground state) by emission of phonons. Thus, the recombination rate is proportional to the excess carrier density, i.e.

$$R_{SRH}^b(t) = A^b n_{tot}(t) \quad (3)$$

where A^b ($A^b > 0$) is a proportionality constant associated to the SRH process. This process is highly detrimental for the performance of optoelectronic devices, as it converts the absorbed energy into the heat.

The third important recombination path, is *Auger recombination*, a tri-molecular process involving a photogenerated e-h pair and a third carrier (electron or hole) carrying out the excess energy. Therefore, the Auger recombination rate has the following for (in the case of third electron):

$$R_{Aug}^b(t) = C^{b1} n_{tot}^2(t) p_{tot}(t) + C^{b2} p_{tot}^2(t) n_{tot}(t) \quad (4)$$

where C^{b1} and C^{b2} are proportionality constants determined by the dynamics of Auger process.

These three recombination paths contribute to the decrease of the excess carrier density, $n(t)$ and $p(t)$. Under high excitation, the excess densities are much higher than the equilibrium densities of both carrier types. Therefore for some initial period ($t > t_o$):

$$n_{tot}(t) \cong n(t) \quad (5a)$$

$$p_{tot}(t) \cong p(t) = n(t) \quad (5b)$$

In this case, the fundamental rate equation describing the optical relaxation, known as ABC equation, is

$$-\frac{dn}{dt} = R_{SRH}^b + R_{rad}^b + R_{Aug}^b = A^b n + B^b n^2 + C^b n^3 \quad (6)$$

The PL intensity $J_{PL}^b(t)$ is proportional to radiative recombination rate $R_{rad}^b(t)$:

$$J_{PL}^b(t) = \Gamma R_{rad}^b(t) = B^b n(t)^2 \Gamma \quad (7)$$

where Γ is the geometric factor of the photodetector. As the relevant information is contained in the time evolution, the PL intensity can be normalized to unity at the initial time t_o , i.e. $J_{PL}^b(t_o) = B^b n_o^2 \Gamma = 1$. Accordingly, Eq. (7) can be written as:

$$J_{PL}^b(t) = \left(\frac{n(t)}{n_o} \right)^2 \quad (9)$$

By division of Eq. (6) by initial carrier density $n(t_o) = n_o$:

$$-\frac{d}{dt} \left(\frac{n}{n_o} \right) = A^b \frac{n}{n_o} + B^b n_o \left(\frac{n}{n_o} \right)^2 + C^b n_o^2 \left(\frac{n}{n_o} \right)^3 \quad (10)$$

Multiplying of both sides of the equation by $2n(t)/n_o$, gives an expression of the time derivative of PL intensity:

$$2 \frac{n}{n_o} \left[A^b \frac{n}{n_o} + B^b n_o \left(\frac{n}{n_o} \right)^2 + C^b n_o^2 \left(\frac{n}{n_o} \right)^3 \right] = -2 \frac{n}{n_o} \frac{dn}{dt} = -\frac{d}{dt} \left(\frac{n}{n_o} \right)^2 = -\frac{dJ_{PL}^b}{dt} \quad (11)$$

Finally, division by the PL intensity J_{PL}^b gives the final result

$$-\frac{1}{J_{PL}^b} \frac{dJ_{PL}^b}{dt} = -\frac{d}{dt} [\ln(J_{PL}^b)] = 2A^b + 2B^b n_o \sqrt{J_{PL}^b} + 2C^b n_o^2 J_{PL}^b \quad (12)$$

which allows a simple determination of the various contributions to carrier relaxation from an Arrhenius plot.

Note that Eq. (12) is only valid for high injection conditions. Therefore, a deviation from the equation is expected for $t > t_o$ when the excess carrier density decreases to a value comparable to equilibrium density of the dominant carrier type. The same situation arises when photogenerated carrier density is much lower than the density of majority carriers at equilibrium. In both cases the total density of majority carriers is approximately equal to equilibrium value, i.e. it is constant, independent of the time.

Under low injection conditions, the total carrier density under excitation can be approximated by:

$$n_{tot}(t) \approx n_{eq} \quad ; \quad p_{tot} = p(t) = n(t) \quad (15a)$$

when the majority carriers are electrons, and

$$p_{tot}(t) \approx p_{eq} \quad ; \quad n_{tot} = n(t) \quad (15b)$$

when the majority carriers are holes. Following Eq. (2), the radiative recombination rate can be approximated by

$$R_{rad}^m(t) = B^b n(t) n_{eq} = A^m n(t) \quad (16a)$$

or

$$R_{rad}^m(t) = B^b n(t) p_{eq} = A^m n(t) \quad (16b)$$

This means that the radiative recombination becomes monomolecular, governed by the excess density of the minority carriers. Note that for long enough time ($t \gg t_0$) the recombination process will always become monomolecular.

On the other hand, the SRH recombination contributes the monomolecular recombination rate, keeping proportional to the carrier density, i.e. $R_{SRH}^m(t) = A^b n(t)$ or $R_{SRH}^m(t) = A^b n(t)$, for electrons or holes as majority carriers, respectively.

Finally, the tri-molecular process, Auger recombination, is described by:

$$R_{Aug}^m(t) = C^m n_{eq}^2 n(t) = A_{Aug}^m n(t) \quad (18a)$$

when the majority carriers are electrons, and

$$R_{Aug}^m(t) = C^m n^2(t) p_{eq} = B_{Aug}^m n^2(t) \quad (18b)$$

when the majority carriers are holes. Hence, in the first case, the Auger recombination adds to monomolecular rate, and in the second it contributes to the bi-molecular recombination. Thus, for low injection, Eq. (6) becomes:

$$-\frac{dn}{dt} = R_{SRH}^m + R_{rad}^m + R_{Aug}^m = (A^b + A^m + A_{Aug}^m)n + B_{Aug}^m n^2 = A_{eff}^m n + B_{Aug}^m n^2 - \quad (19)$$

As previously, the PL intensity $J_{PL}^m(t)$ is proportional to radiative recombination rate $R_{rad}^m(t)$ and the geometric factor Γ :

$$J_{PL}^m(t) = \Gamma R_{rad}^m(t) = A^m n(t) \Gamma \quad (20)$$

and the geometric factor Γ can be removed by normalizing PL intensity by its value at the initial time:

$$J_{PL}^m(t) = \frac{n(t)}{n_o} \quad (21)$$

Both sides of Eq. (19) are divided by n_o and by the PL intensity $J_{PL}^m(t)$ to arrive to the final expression:

$$-\frac{d[\ln(J_{PL}^m)]}{dt} = A_{eff}^m + B_{Aug}^m n_o J_{PL}^m \quad (22)$$

Note the similarity of the derived expression for high injection and low injection in Eqs (12) and (22), respectively. Therefore, it is possible to extract the coefficients associated with the different recombination processes from a common parabolic dependence:

$$F(y) = \alpha + \beta y + \lambda y^2 \quad (23)$$

where these factors depend on the type of the process:

$$\text{- High injection: } y = \sqrt{J_{PL}^b}, \quad \alpha = 2A^b, \quad \beta = 2B^b n_o, \quad \lambda = 2C^b n_o^2 \quad (24a)$$

$$\text{- Low injection: } y = J_{PL}^m, \quad \alpha = A_{eff}^m, \quad \beta = B_{Aug}^m n_o, \quad \lambda \approx 0 \quad (24b)$$

As shown in Fig. 1 (a), the terminating stage of high excitation, corresponds to transition to Process II characterized by linear dependence of PL intensity, i.e. Eq. (14) relation is not fulfilled. Using relation $J_{PL}^m = K(\sqrt{J_{PL}^b})^2$, the following

$$-\frac{d[\ln(J_{PL}^m)]}{dt} = A + B n_o K (\sqrt{J_{PL}^b})^2 + C n_o^2 K^2 (\sqrt{J_{PL}^b})^4 \quad (25)$$

i.e. in the part of diagram corresponding to Process II, plotted in Fig. 1a, the dependence on $\sqrt{J_{PL}^b}$ should be bi-quadratic, i.e.

$$F(y) = \alpha + \beta y^2 + \gamma y^4 \quad (26)$$

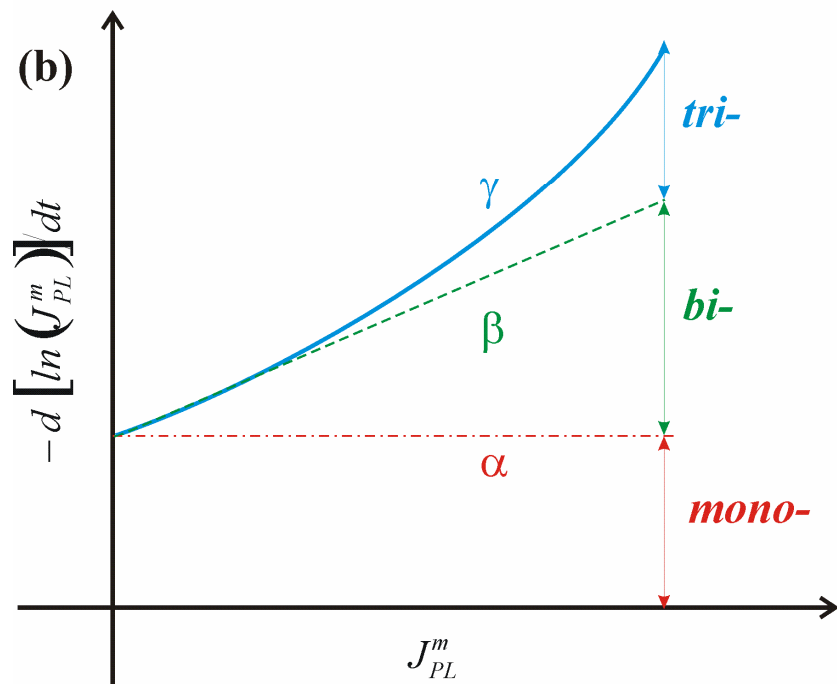
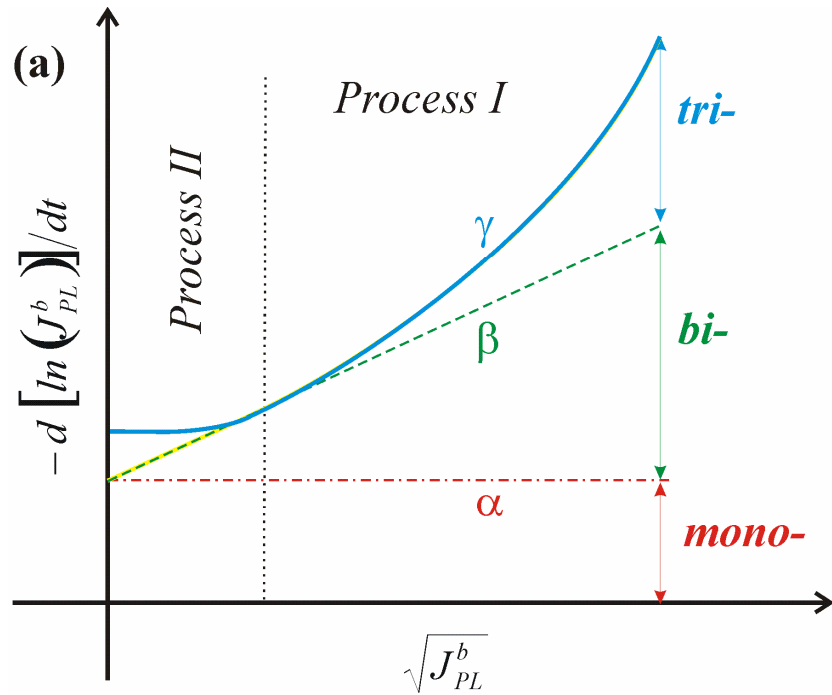


Fig. 1. Logarithmic time derivative of PL intensity for two different excitation levels: (a) for high excitation as a function of square root of PL intensity, (b) for low excitation as a function of PL intensity. High excitation regime time evolution (a) is divided by vertical dotted line into process I (Eq. (23)) and process II (Eq. (26)). The red dash-dotted, green dotted and solid blue line correspond to the evolution according to α , $\alpha + \beta$ and $\alpha + \beta + \gamma$ parameters. The values of the parameters are: $\alpha = 1$, $\beta = 2$ and $\gamma = 3$. The relative weight of the various molecular processes at the initial level is marked by arrows for $J = 1$.

Note that the implementation of the above presented procedure requires needs several stringent conditions to be met. First, that the averaged PL intensity should drop to zero for long times. Finally, it has to be stressed that the ABC model is a mere approximation of the more complex phenomena of optical relaxation, so that a deviation is likely to be detected.

III. Application to GaN/AlN multi-quantum-wells

As an example, we present here the analysis of the TRPL from a GaN/AlN multi-quantum-well (MQW) structure grown on an AlN-on-sapphire substrate by plasma-assisted molecular beam epitaxy (PA-MBE). The MQW stack consists of 40 periods of 1.5-nm-thick GaN wells and 4-nm-thick AlN barriers. The GaN layers were doped with Si to a concentration of $1.3 \times 10^{19} \text{ cm}^{-3}$. A scanning transmission electron microscopy (TEM) view of the MQW is presented in Fig. 2. The picture proves that the thicknesses of barrier/wells are almost uniform with low density of extended defects.

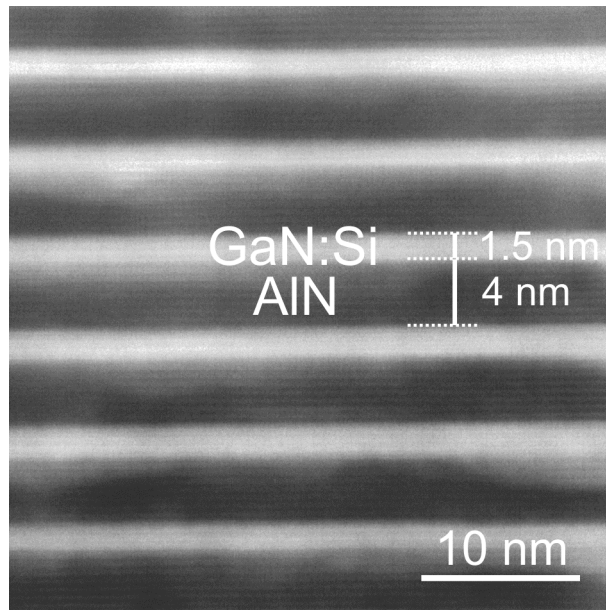


Fig. 2. Cross-sectional HAADF-STEM image of 1.5-nm-thick GaN wells with 4 nm-thick AlN barriers the GaN/AlN MQW structure.

Photoluminescence was excited with third harmonic of Ti:Sapphire pulsed laser ($\lambda = 300$ nm, $f = 80$ MHz). The light beam was analyzed by spectrometer and directed on a CCD detector and streak camera. The streak camera enabled time-resolved measurements.

The first step is determination of the dominant process type. This can be achieved by plotting the PL intensity versus excitation laser power, as shown in Fig. 3. Naturally, the variation of the laser excitation should be limited so that the measurement conditions are similar to the TRPL measurements.

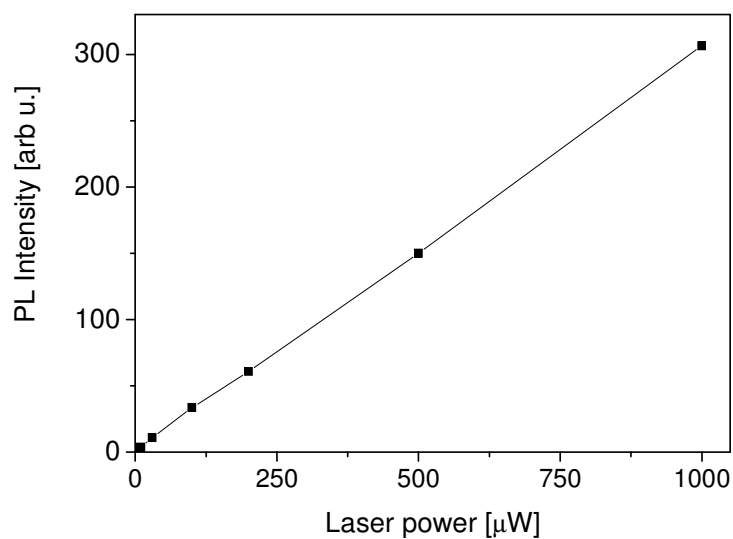
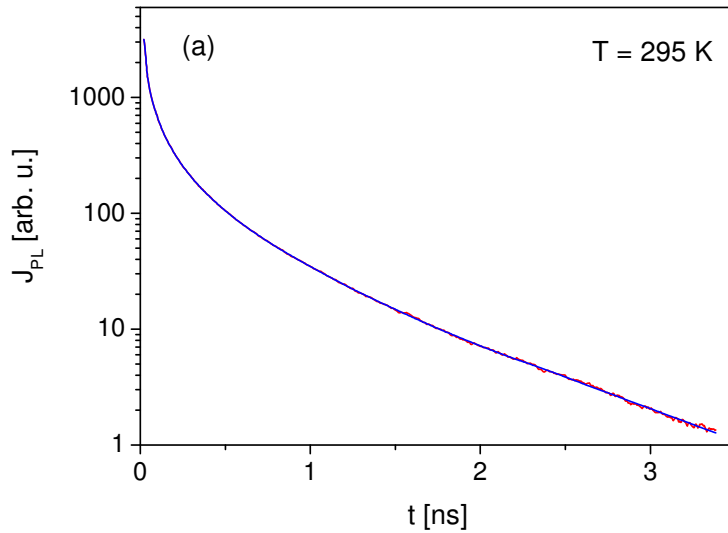


Fig 3. The integrated PL intensity of polar nitride MQW structure as a function of the excitation laser power.

From the graph it follows that the optical response to laser excitation is linear. Thus in analysis of the optical emission Eq. (22) applies.

The logarithmic plot of PL intensity versus time is shown in Fig. 4. As it is shown the initial part strongly deviates from straight line, indicating the domination of the two- or three-carrier recombination processes. The decay is closer to exponential (straight line in logarithmic scale) for the terminal phase time evolution, confirming the dominant mononuclear emission.



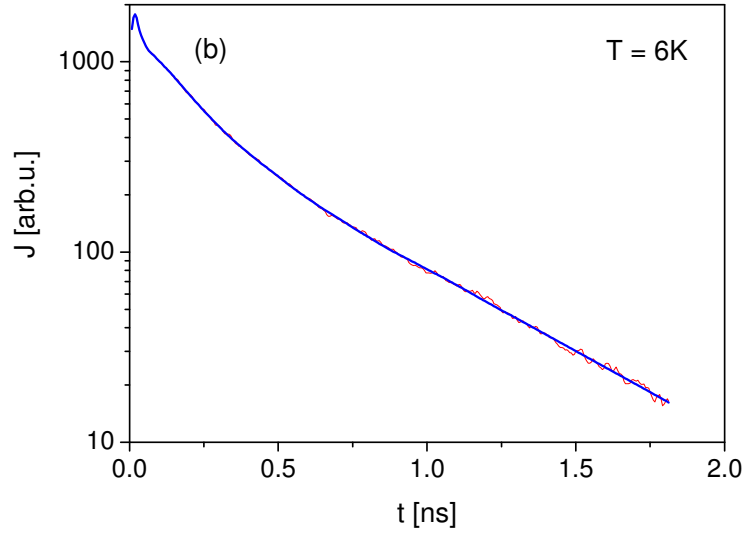


Fig 4. PL time decay of polar (a) and nonpolar (b) nitride MQW structures. The red line – raw signal with the background subtracted, the blue line – noise averaged line. The polar and nonpolar signals were collected in the (3.3738 eV, 3.8978 eV) and (3.5233 eV, 3.5564 eV) intervals, respectively. The dominant emission peaks were located within these intervals during entire measurement time. The laser power was 1000 μ W, the excitation length 300 nm.

Note that the signal is burdened by considerable noise, which is partially related to thermal fluctuation of the density of electron-hole (e-h) pairs, and partially to the electronic noise in the collecting device.

In order to obtain the logarithmic time derivative of the signal, the noisy signal has to be replaced by C^1 approximation. The procedure of such averaging may be different: in the present case the approximation by the local least-square approximation was adopted. The averaged time dependence is also shown in Fig. 4.

From the noise-averaged time dependence the logarithmic derivative of the PL intensity – $\frac{d[\ln(J)]}{dt}$ as a function of the intensity J was obtained. The dependence is plotted in Fig 5 along with the approximate relation given by Eq. (26).

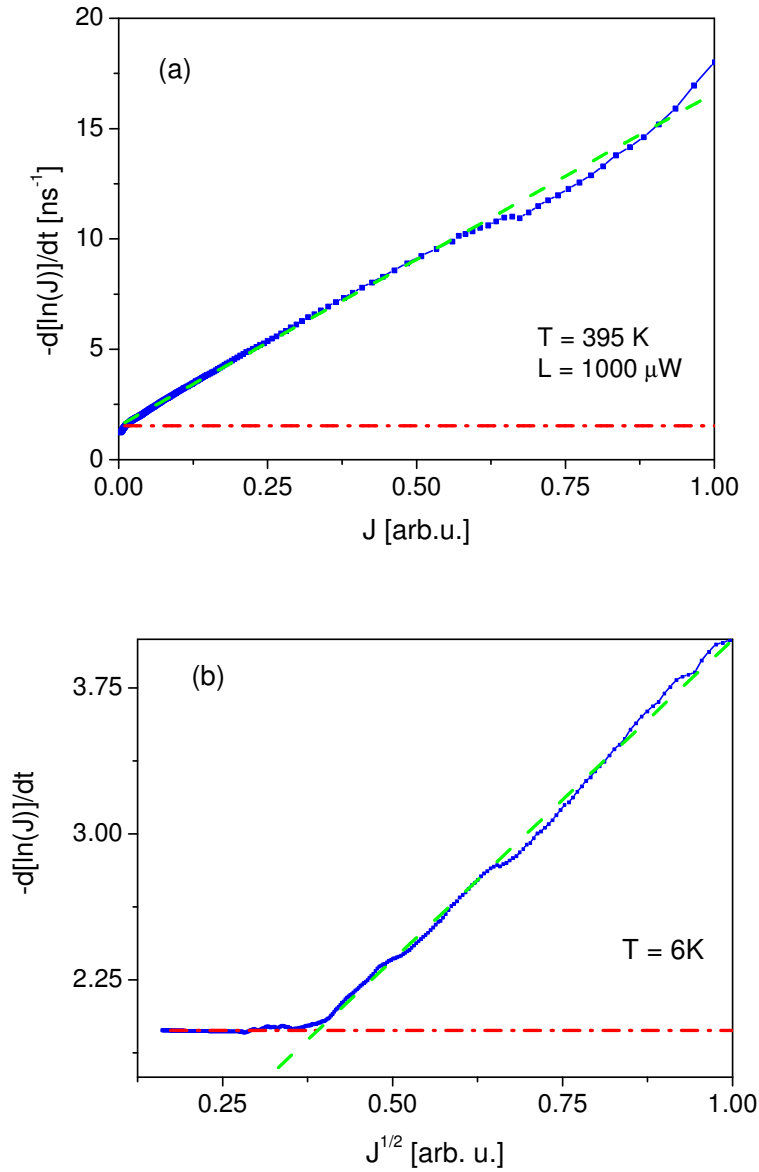


Fig 5. Logarithmic time derivative as a function of the intensity of the normalized PL intensity from polar nitride MQW structure at room temperature (a) and 6 K (b) (blue symbols and solid line). The red dash-dotted line represents constant value α , the green dashed line – the linear approximation $\alpha + \beta J$.

For the high temperature PL from polar MQWs (fig 5a) the coefficient α determining the monomolecular process is determined to $\alpha^m = A^m = 1.53 \text{ ns}^{-1}$. Thus the linear relaxation time is $\tau^m = 0.65 \text{ ns}$. The second parameter was $\beta^m = B^m n_o = 15.1 \text{ ns}^{-1}$. This indicates the dominance of the bi-molecular recombination in the process which attains one order of magnitude higher than the monomolecular term. The reference initial value was determined

to $J = 1226$ in the normalized units used in Fig. 5. The third order term is negligible. As it is also shown, the quality of the time evolution curve is crucial for the successful determination of these contribution. It may be observed that in Fig. 5a, for the diagram part above 0.6 in normalized PL intensity, the nonlinear part is visible. This part may have approximate coefficient $\gamma = Cn_o^2 = 3.4 \text{ ns}^{-1}$, which may be also signature of transition to nonlinear regime in PL intensity.

For the nonpolar MQWs measured at 6 K, the coefficient α determining the monomolecular process is determined to $\alpha^b = 0.71 \text{ ns}^{-1}$. That translates to the coefficient $A^b = 0.36 \text{ ns}^{-1}$. The linear relaxation time is $\tau = 2.77 \text{ ns}$. The second parameter was $\beta^b = 3.29 \text{ ns}^{-1}$ from which the value of parameter B could be obtained $B^b n_o = 1.65 \text{ ns}^{-1}$. Again the nonlinear term dominates. The nonlinear Auger related contribution is negligible.

IV. Summary

The above presented results may be summarized as follows:

- New method of analysis of TRPL data was proposed, based on the dependence of logarithmic time derivative of the PL intensity as a function of the same PL intensity.
- The method is based on exact transformation avoiding any approximations.
- The noise reduction scheme is critical to the successful application of the method.
- The method provides graphic representation of the results allowing identification of the mono, bi-, tri- and higher order recombination processes.
- The method could be used to determine standard ABC constant and higher order parameters in more specific processes.
- Application of the method may be universal to analysis of the PL decay of any system, semiconducting, molecular etc.
- The method may precisely verify various models of efficiency droop in nitride structures.

- In the exemplary GaN/AlN system, the method identifies the value of A constant, the bi-molecular B parameter, negligible contribution of higher order processes, including Auger recombination. .

References

- ¹G.F.J. Garlic, *Luminescence*, in *Light and Matter II*, G. Flugge (ed), Springer-Verlag, Berlin-Heidelberg 1958, p. 1
- ²V.H.B. Bebb, and E.W. Williams, *Photoluminescence I. Theory*, in *Semiconductors and Semimetals*, R.K. Willardson and A. C. Beer (eds), Academic Press, New York 1972, Vol. 8, p. 181
- ³V. P. Gribkovskii, *Theory of Luminescence*, in *Luminescence of Solids*, D. R. Vij (ed), Plenum Press, New York, 1998.
- ⁴I. Pelant, J. Valenta, *Luminescence Spectroscopy of Semiconductors*, Oxford Univ. Press, Oxford
- ⁵S. M. Sze, *Physics of Semiconductor Devices*, Wiley, New York, 2001.
- ⁶W. Shockley, W. T. Read, Jr. *Phys. Rev.* 87, 835 (1952).
- ⁷G.H. Wannier, *Phys. Rev.* 52, 191 (1937).
- ⁸N. F. Mott, *Trans. Faraday Soc.* 34, 500 (1938).
- ⁹M. H. Anderson, J. R. Ensher, M. R. Matthews, C. E. Wieman, and E. A. Cornell, *Science*, 269, 198 (1995).
- ¹⁰S. Schmitt-Rink, D.S. Chemla, and D. A. B. Miller, *Phys. Rev. B.* 32, 6601 (1985).
- ¹¹E. Zielinski, F. Keppler, S. Hausser, M. H. Pilkuhn, R. Sauer, and W. T. Tsang, *IEEE J. Quant. Electron.* 25, 1407 (1989).
- ¹²M. F. Schubert, S. Chhajed, J. K. Kim, E. F. Schubert, D. D. Koleske, M. H. Crawford, S. R. Lee, A. J. Fischer, G. Thaler, and M. A. Banas, *Appl. Phys. Lett.* **91**, 231114 (2007)

- ¹³Q. Dai, Q. Shan, J. Weng, S. Chhajed, J. Cho, E. F. Schubert, M. H. Crawford, D. D. Koleske, M.-H. Kim, and Y. Park, *Appl. Phys. Lett.* 97, 133507 (2010).
- ¹⁴M. G. Brik, S. Mahlik, D. Jankowski, P. Strak, K. P. Korona, E. Monroy, S. Krukowski, and A. Kaminska, *Jpn. J. Appl. Phys.* 56, 05FA02 (2017).
- ¹⁵F. Wootan, *Optical Properties of Solids*, Academic Press, New York, 1972.
- ¹⁶M. Inokuti and F. Hirayama, *J. Chem. Phys.* 43, 1978 (1965).
- ¹⁷M. Millot, Z. M. Geballe, K. M. Yu, W. Walukiewicz, and R. Jeanloz, *Appl. Phys. Lett.* 100, 162103 (2012).
- ¹⁸S. Chichibu, T. Azuhata, T. Sota, S. Nakamura, *Appl. Phys. Lett.* 69, 4188, (1996).
- ¹⁹S. Chichibu, T. Azuhata, T. Sota, S. Nakamura, *Appl. Phys. Lett.* 70, 2822 (1997).
- ²⁰S. F. Chichibu, A. Uedono, T. Onuma, B. A. Haskell, A. Chakraborty, T. Koyama, P. T. Fini, S. Keller, S. P. Denbaars, J. S. Speck, U. K. Mishra, S. Nakamura, S. Yamaguchi, S. Kamiyama, H. Amano, I. Akasaki, J. Han, T. Sota, *Nature Mater.* 5, 810 (2006).
- ²¹R. A. Oliver, S. E. Bennett, T. Zhu, D. J. Beesley, M. J. Kappers, D. W. Saxey, A. Cerezo, C. J. Humphreys, *J. Phys. D: Appl. Phys.* 43, 354003 (2010).
- ²²F. Bernardini, V. Fiorentini, and D. Vanderbilt, *Phys. Rev. Lett.* 79, 3958 (1997).
- ²³A. Kaminska, P. Strak, J. Borysiuk, K. Sobczak, J. Z. Domagala, M. Beeler, E. Grzanka, K. Sakowski, S. Krukowski, E. Monroy, *J. Appl. Phys.* 119, 015703 (2016).
- ²⁴P. Strak, P. Kempisty, K. Sakowski, A. Kaminska, D. Jankowski, K. P. Korona, K. Sobczak, J. Borysiuk, M. Beeler, E. Grzanka, E. Monroy and S. Krukowski, *AIP Advances* 7 015027-1-26 (2017).
- ²⁵P. Strak, P. Kempisty, K. Sakowski, and S. Krukowski, *J. Cryst. Growth*, 401, 652 (2014).
- ²⁶A. Suchocki, J. M. Langer, *Phys. Rev. B* 39, 7905 (1989)
- ²⁷S. Hausser, G. Fuchs, A. Hangleiter, K. Streubel, and W. T. Tsang, *Appl. Phys. Lett.* 56, 913 (1990).
- ²⁸J. Cho, E. Schubert, and J. Kim, *Laser Photon. Rev.* 7, 408 (2013).

²⁹M. Shahmohammadi, W. Liu, G. Rossbach, L. Lahourcade, A. Dussaigne, C. Bougerol, R. Butte, N. Grandjean, B. Deveaud, and G. Jacopin, *Phys. Rev. B* **95**, 125314 (2017).

³⁰M. R. Krames, G. Christenson, D. Collins, L. W. Cook, M. G. Craford, A. Edwards, R. M. Fletcher, N. F. Gardner, W. K. Goetz, W. R. Imler, E. Johnson, R. S. Kern, R. Khare, F. A. Kish, C. Lowery, M. J. Ludowise, R. Mann, M. Maranowski, S. A. Maranowski, P. S. Martin *et al.*, *Proc. SPIE* **3938**, 2 (2000).

³¹T. Mukai, M. Yamada, and S. Nakamura, *Jpn. J. Appl. Phys.* **38**, 3976 (1999).